ISSN 2347 - 3983
Volume 8. No. 7, July 2020
International Journal of Emerging Trends in Engineering Research
Available Online at http://www.warse.org/IJETER/static/pdf/file/ijeter172872020.pdf
https://doi.org/10.30534/ijeter/2020/172872020

High-Rise Building Wind Analysis Using Computational Fluid Dynamics and Dynamic Analysis Using ETABS Program

W. S. Karrar, A. M. Shyama, M. Jassim
[1]Engineer, Department of Civil, College of Engineering, Mustansiriyah, Iraq, seerbeenkarar@gmail.com
[2]Associate Professor Doctor, Department of Water Resource, College of Engineering, Mustansiriyah University, Iraq, shyabed1976@gmail.com
[3]Lecture Doctor, Department of Civil, College of Engineering, Mustansiriyah University, Iraq, Jassim_Muhsin@yahoo.com

ABSTRACT

Present paper is devoted to study wind load on tall building. Computational fluid dynamic (CFD) model was performed in three-dimensional (3D) commercial packages ANSYS (Fluid Fluent) 19.0. Utilizing finite volume technique to predict the wind load on tall building using specific boundary conditions. LES and standard k-ε turbulence model were used in the program to consider the wind turbulence. Current numerical approach was verified by comparison the drag coefficient and left coefficient results with experimental wind tunnel tests. This valid CFD model was applied in the simulation of the wind analysis for theoretical building, which is assumed located in Baghdad City, Iraq. It is connected that wind load results of CFD have a good agreement with the wind load results of building codes. This building was dynamically analyzed and good results were obtained.

Key words: Tall Buildings, Finite Volume Method, Computational Fluid Dynamic (CFD), Standard κ-ε Turbulence Model, LES, Wind Pressure on Building.

1. INTRODUCTION

Each nation utilized its building code [ASCE: 7-02 (2002), AS/NZS: 1170.2 (2002), the Euro code, BS-EN 1991-1-4 (2005), IS 875-Part 3 (1987) and so on.]. With regard to the building codes, there is a common denominator which that all of them are using approximate, yet in particular safe approach, that consists of practical suggestion for determining wind load on the structure. An approach which impacts influential parameters have been divided between coefficients, factors, as well as reference values has been regularly distinctive for each one of the codes. With regard to many terrain characteristics, roughness height z^o in addition to friction velocity u* has been provided in the building code. With such properties, 10min-averaged or hourly-averaged wind velocity profile with specific repetition time has been specified. Usually, such velocity has been exceeded just one time. In the case when structures have been created on ultimate limit state; there has been a requirement for determining the anticipated maximum value regarding the pressure on façade, including the impact regarding the wind's gustiness. Such impact has been included with regard to factor on the basis of turbulence intensity that is related to approaching flow. The highest dynamic pressure has been evaluated with factors which were indicated earlier for account for dependency on terrain, height as well as position. Following determining extreme dynamic pressure, loads on structure or even just part of it might be specified with the use of representative area, also coefficients which are account for structure's shape. Benefits regarding this approach are that calculations can be considered useful through all phases regarding the building process, calculations can be easily repeated, reproduced, extremely reliable also the time needed for calculation is low. This method's drawbacks are that the codes aren't utilized for all the building shapes, simplistic rules are used via codes, that aren't constantly precise, also flow field around the building cannot be evaluated. This can be considered as latest approach for determining the wind loading on the structures. CFD applies numeric for determining fluid's flow in specific domain, such method is operating on the basis of Navier-Stokes equations, that is considered as derivation with regard to the indications of Newton and Euler of the next 3-conservation rules, conservation of momentum, conservation of energy, as well as the conservation of mass. Computational domain has been discretized spatially, also Navier-Stokes equations have been discretized numerically, and set-up for each one of the cell volumes. Furthermore, wind tunnel technique in addition to building code, the representative wind velocity has been translated in to the representative pressure on (part of) the structure. Such pressure is inducing mechanical responses with regard to structure that will be checked on the basis of

specific standard. In the case of meeting the standards, the structure will be fulfilling the requirements in terms of wind loading. The profile that is related to representative velocity, terrain characteristics regarding zo as well as u* have been incorporated. The approach in which turbulence has been incorporated in the approach is on the basis of distinctive simulation approaches. The major benefit regarding such approach are that the simulation could be early utilized in building process, simulations could be repeated easily, simulations can be controlled easily , also flow field around building could be determined easily. The drawbacks regarding such approach are numerical techniques are regularly limited through computer capacity, the approaches are providing numerical errors, the approaches are requiring significant modelling that will be introducing errors and results were badly verified. [10] examined comparison related to the wind load on building used design codes, wind tunnel tests and CFD. Two building models were used in this study. The dimensions of the two building were (25x15x45 m) and (55x45x200 m). After calculated the wind loads on buildings. he concluded that the estimated wind loads on buildings by using CFD is comparable with the results by wind tunnel test and those by building design codes are more conservative than the CFD and wind tunnel test. [4] examined the building model of Commonwealth Advisory Aeronautical Council (CAARC) which has dimensions of (30mx45mx183m) in the wind analysis. Such work has been on the basis of numerical approach with focus on the equations of Reynolds Averaged Navier Stokes (RANS) as well as the turbulence model of Large Eddy Simulation (LES). The pressures of wind on tall building have been estimated and put to comparison with wind tunnel measurement with regard to buildings. Re-normalized group RNG k-ε turbulence model are providing more effective accordance regarding the boundary layer wind tunnel results in comparison to standard k-ε. The matching of turbulent model was indicated between LES numerical results as well as experimental results on the windward face. At the same time, the agreement deteriorated to some extent at sidewalls and enhanced at leeward wall. [3] examined the computational evaluations with regard to the wind loads on high as well as lo rise buildings. The model's dimensions have been (30.48mx45.72mx182.88m). All results have been put to comparison as well as being verified with the experimental data. With adequate modeling which represent in realistic way the actual turbulent atmospheric boundary layer flows, CFD has the ability of providing economical alternatives to current wind engineering approaches. The easy accessibility of CFD has been anticipated for transferring the practice that is related to the wind's structural design, causing extra wind-resilient in addition to sustainable systems through inducing optimal aerodynamic, also sustainable structural/building designs. Therefore, this approach is going to enable ensuring public safety as well as reducing the economic loss because of wind damage. [2] studied the impact of the wind on tall building through using CFD simulation. The researcher utilized numerical algorithms as well as turbulence modeling with the use of RANS and LES equations utilized to square prismatic prototype structures as well as studying the model's dynamic properties. The dimensions of model were (40x40x300 m). Wind tunnel scale has been selected to be (1:400), and this decreased the dimensions to be (0.1mx0.1mx0.75m). The researcher indicated that the mean pressure values specified comparative agreements with the published data as well as the industry accepted design codes and might be utilized in simulations of CFD as alternative tool with regard to the wind pressure loading for pre-design stages of tall structure projects. [12] provided CFD's simulation which has been conducted in 3-D with regard to the wind analysis regarding Rixos Hotel (Duhok City, Iraq). The building of Rixos Hotel, that has been built with reinforced concrete of height (80m). RNG k-ε turbulence model, has been applied in analysis for considering wind turbulence. Present numerical method has been proved through comparing the results with the experimental wind tunnel tests. CFD simulation that is related to the analysis outputs regarding Rixos building have been compared to those determined through certain international building codes; agreement has been indicated with the use of ASCE 2010 code. The work indicated that the current 3-D steady CFD simulation method might be applied as alternate approach for overpriced wind tunnel methods with reasonable correlation coefficient with regard to the simulation related to wind flow around irregular buildings. Streamline velocity that is related to the wind flow in CFD's simulation at two thirds regarding the height of building come to rest and make stagnation point. ASCE standard with regard to the wind pressure measurements have been matched with CFD simulation results regarding wind analysis for the concrete high buildings in Duhok city.

2. GOVERNING EQUATIONS FOR WIND

The governing equations in fluid dynamics can be applied to wind flow. Liquid or wind flows in CFD codes are governed by partial differential equations, which are based on the conservation laws for mass, energy and momentum. The following expressions are applied for three dimensional, steady and incompressible flows with constant viscosity.

$$\frac{\partial \rho}{\partial t} + \left[\frac{\partial(\rho u)}{\partial x} + \frac{\partial(\rho v)}{\partial y} + \frac{\partial(\rho w)}{\partial z}\right] = 0 \qquad (1)$$

$$\rho \frac{Du}{Dt} - -\frac{\partial \rho}{\partial x} + \frac{\partial \tau_{xx}}{\partial x} + \frac{\partial \tau_{yx}}{\partial y} + \frac{\partial \tau_{zx}}{\partial z} + \rho f_x \qquad (2\text{-x})$$

$$\rho \frac{Dv}{Dt} - -\frac{\partial \rho}{\partial y} + \frac{\partial \tau_{yy}}{\partial y} + \frac{\partial \tau_{yx}}{\partial x} + \frac{\partial \tau_{zy}}{\partial z} + \rho f_y \qquad (2\text{-y})$$

$$\rho \frac{Dw}{Dt} = \frac{\partial \rho}{\partial z} + \frac{\partial \tau_{zz}}{\partial z} + \frac{\partial \tau_{yz}}{\partial y} + \frac{\partial \tau_{xz}}{\partial x} + \rho f_z \qquad (2\text{-z})$$

$$\tau_{xy} = \tau_{yx} = \mu(\frac{\partial v}{\partial x} + \frac{\partial u}{\partial y})$$

$$\tau_{xz} - \tau_{zx} - \mu(\frac{\partial w}{\partial x} + \frac{\partial u}{\partial z})$$

$$\tau_{zy} = \tau_{yz} = \mu(\frac{\partial v}{\partial y} + \frac{\partial w}{\partial y})$$

$$\tau_{xx} - -\frac{2}{3}\mu(\nabla . V) + 2\mu\frac{\partial u}{\partial x}$$

$$\tau_{yy} = -\frac{2}{3}\mu(\nabla . V) + 2\mu\frac{\partial v}{\partial y}$$

$$\tau_{zz} - -\frac{2}{3}\mu(\nabla . V) + 2\mu\frac{\partial w}{\partial z}$$

$$\rho\frac{D}{Dt}\left(e + \frac{V^2}{2}\right) = \rho q + \frac{\partial}{\partial x}\left(k\frac{\partial T}{\partial x}\right) + \frac{\partial}{\partial y}\left(k\frac{\partial T}{\partial y}\right) + \frac{\partial}{\partial z}\left(k\frac{\partial T}{\partial z}\right) - \frac{\partial(up)}{\partial x}$$

$$-\frac{\partial(vp)}{\partial y} - \frac{\partial wp}{\partial z} + \frac{\partial(u\tau_{xx})}{\partial x} + \frac{\partial(u\tau_{yx})}{\partial y} + \frac{\partial(u\tau_{zx})}{\partial z} + \frac{\partial(v\tau_{xy})}{\partial x} + \frac{\partial(v\tau_{yy})}{\partial y} + \frac{\partial(v\tau_{zy})}{\partial z} + \frac{\partial(w\tau_{xz})}{\partial x} + \frac{\partial(w\tau_{yz})}{\partial y} + \frac{\partial(w\tau_{zz})}{\partial z} + \rho f . V \quad (3)$$

Where; ρ is density of fluid in Kg/m^3, u, v and w velocities of fluid in x, y and z directions respectively in m/s, τ is the shear stress in Pa, t is the time in s, f_x, f_y and f_z are the body forces in N, μ is the molecular viscosity coefficient in Pa.s, V is velocity vector in m/s, k is the thermal conductivity, e is the internal energy in J , T is the temperature in C^o and q is the heat transferred *W/m²·K*.

3. THE STANDARD K-E MODEL

κ-ε model is focused on approaches affecting the turbulent kinetics energy. It should be taken under consideration that k stands for the turbulent kinetics energy, and ε stands for turbulent rate of dissipation. The 2-equation model of turbulence provides the ability to determine both, the turbulent length and the time scale through the solution of 2 distinct equations of the transport. The model of the k-ε can be defined in a model class, which became the practical engineering problems workhorse due to the fact that it has been suggested in 1974 by Spalding and Launder [7].

The conventional k-ε model has been modeled on the basis of the transport equations. For turbulence kinetics energy (k) and its rate of dissipation (ε). k eq. has been derivative from exactness; none-the-less, an equation of the model transportation for (ε) has been produced through the physical reasoning and pays no significant similarity with its immediate counterpart. The turbulence kinetic energy transport equations, κ, and its dissipation rate, ε, can be characterized as:

$$\frac{\partial}{\partial t}(\rho k) + \frac{\partial}{\partial x_i}(\rho k u_i) = \frac{\partial}{\partial x_i}\left[\left(\mu + \frac{\mu_T}{\sigma_k}\right)\frac{\partial k}{\partial x_i}\right] + G_k + G_b + S_k - \rho\varepsilon - Y_M \quad (4)$$

$$\frac{\partial}{\partial t}(\rho\varepsilon) + \frac{\partial}{\partial x_i}(\rho\varepsilon u_i) - \frac{\partial}{\partial x_i}\left[\left(\mu + \frac{\mu_i}{\sigma_F}\right)\frac{\partial\varepsilon}{\partial x_i}\right] + C_{1\varepsilon}\frac{\varepsilon}{k}(G_k + C_{3\varepsilon}G_b) - C_{2\varepsilon}\rho\frac{\varepsilon^2}{k} + S_\varepsilon \quad (5)$$

In those equations. G_k, stands for turbulence kinetic energy generation as a result of the average gradients of the velocity, which are computed through by referring to the turbulent production model in k-ε models. G_b represents a generation of the turbulence kinetic energy due to buoyancy. Y_M is fluctuating dilatation contribution in compressible turbulence to general rate of dissipation. $C_{1\varepsilon}$, $C_{2\varepsilon}$, $C_{3\varepsilon}$, are the constants, which are equal to 1.440, 1.920, 0.090, respectively; σ_k, σ_ε represent the numbers of Prandtl for k and ε with respectively 1 and 1.30 values. S_k and S_ε represent the user defined terms of the source. Those values were specified from the basic experimentations for the turbulent flow that have been encountered often in the shear flows such as the boundary layers. They were discovered to work rather efficiently for numerous free shear and wall-bounded flows [9].

4. SST K-Ω MODEL

The k-ω model of the shear-stress transport (SST) has been advanced by [11] for an effective addition of precise and strong formulation in the near-wall area with the free stream which is not dependent on the k-ε model in the extreme fields. This model can be considered equivalent to standard model, however, it comprises the refinements below:

1) The model of the SST includes a derivative term of the damped cross-diffusion in ω equation.

2) The standard and transformed k-ε models are multiplied with a function of blending and after that, they are combined. The function has been designed for having a value which is equal to 1 in near wall area, and 0 in a distance from surface.

3) In those models, the constants have various values.

4) The turbulent viscosity definition is adjusted for accounting for shear stress transport.

The main manner by which the model of the SST is different from conventional model are in the following manner: (a) the gradual changes from conventional k-ω model in inner boundary layer region to a high k-ε model Reynolds number in the external boundary layer part, and (b) the altered turbulent formulation of viscosity for accounting for effects of transportation of main turbulent shear stress. Those lineaments produce an SST (k-ω) model additional dependable and precise for a broader flows category.

$$\frac{\partial}{\partial t}(\rho k) + \frac{\partial}{\partial x_i}(\rho k u_i) = \frac{\partial}{\partial x_j}\left(\Gamma_k\frac{\partial k}{\partial u_j}\right) + G_k + S_k - Y_k \quad (6)$$

$$\frac{\partial}{\partial t}(\rho\omega) + \frac{\partial}{\partial x_j}(\rho\omega u_j) = \frac{\partial}{\partial x_j}\left(\Gamma_\omega \frac{\partial \omega}{\partial u_j}\right) + G_\omega + S_\omega - Y_\omega + D_\omega \quad (7)$$

In the equations above, Gk, stands for the turbulence kinetics energy generation as a result of the mean gradients of the velocity. Γ_k and Γ_ω stand the respective sufficient k and ω diffusivity, G_ω stands for ω generation, Y_k stands for the k dissipation and Y_ω stands for ω dissipation as a result of the turbulence. D_ω stands for the term of the cross-diffusion. Those terms are of specified models that are related to them, which are left for the referencing of the reader. Finally, S_k and Sω represent the user defined source terms [9].

The turbulence modelling field offers a wide range of the research activities for communities of engineering and CFD. Formulations of RANS which have been stated in the present section are commonly available in the commercially available programming codes. Specialists of industry have been extensively using those concepts and gave good results despite the observations which are related to the limited abilities that it has [7]. In this research, the model of the SST k-ω has been used for to model wind flow around bluff body.

5. LARGE EDDY SIMULATION

Another method for the calculation of the turbulent flows is accepting for the fact that larger eddies are required to be calculated for every one of the problems with time-dependent simulation. The smaller eddies' universal behavior has to be captured easier with the compact model. Rather than the time averaging, LES utilizes the spatial filtering for the separation of larger eddies from the smaller ones. This approach utilizes the filtering function selection and a specific length scale of the cutoff aiming to resolve in a computation of the unsteady flow all these eddies which are of higher scale of length compared to the dimension of the cutoff. Throughout spatial filtering, information which is associate with smaller eddies below the length of the cutoff is eliminated. The velocity spectrum is presented in Figure 1. This effect of the interaction between the larger eddies and the smaller ones result in the sub-grid-scale (SGS) stresses. This can be considered as the main large eddy simulation (LES) concept method for numerically treating and solving him turbulence in the fluids [7].

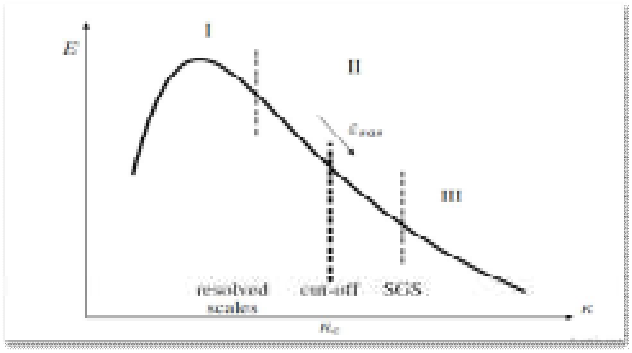

Figure 1: Velocity Spectrum. [5]

The explanation for the LES may be explained as: (a) mass, momentum, energy and other scalars are moved with the larger eddies, (b) the larger eddies are problem-dependent; which means that they're regulated with the boundary and the geometry flow conditions, (c) smaller eddies aren't dependent upon the geometry, which means that they're isotropic. Through the resolution of larger eddies, they have to utilize the finer meshes compared to the ones that are utilized in the models of the RANS. LES must be run usually for long periods for the sake of obtaining the stable statistics for flow which is being modeled [9]. Which is why, the time of the computation is longer and high-performance computing (HPC) can be considered as a must for the simulations of the LES. The drawback regarding to LES lies in high-resolution wall boundary layer requirements due to the fact that near the wall, the even larger eddies become smaller and need a Reynolds number dependent solution. Usually, the LES is limited to the Reynolds numbers in ranging from 10^4 to 10^5 and smaller scopes of the computation.

A considerable part of the is a result of the transport of the convective momentum as a result of the interactions between unresolved eddies that are known as the sub grid-scale stress. The turbulence models of the sub grid-scale typically use the hypothesis of the Boussinesq [8]. The sub grid-scale turbulent stresses are calculated based on:

$$\tau_{ij} - \frac{1}{3}\tau_{kk}\delta_{ij} = \mu_t S_{ij} \quad (8)$$

For the compressible flows, there is a necessity for introducing the Favre (i.e. the density-weighted) refinement operator. The compressible sub-grid stress tensor form can be characterized through dividing it to its deviatoric part and isotropic part

$$\tau_{ij} = \tau_{ij} - \frac{1}{3}\tau_{kk}\delta_{ij} + \frac{1}{3}\tau_{kk}\delta_{ij} \quad (9)$$

Where the subgrid-scale stress tensor's deviatoric part is molded with the use of compressible Smagorinsky model form [9].

$$\tau_{ij} - \frac{1}{3}\tau_{kk}\delta_{ij} = -2\,\mu_t\left(S_{ij} - \frac{1}{3}S_{kk}\delta_{ij}\right) \quad (10)$$

This model has been developed initially by [13]. Eddy-viscosity can be modeled as;

$$\mu_t = \rho\, L_s^2 |S| \quad (11)$$

Where L_s is sub-grid scales' mixing length and $|S| - \sqrt{2}\, S_{ij}\, S_{ij}$ and L_s may be computed using;

$$l_s = \min(kd, C_s\Delta) \quad (12)$$

k represents von Kármán constant which is approximately equal to 0.41, d represents distance to nearest wall, Cs represents constant of Smagorinsky, and Δ represents scale of the local grid according to element volume. Researcher Lilly has obtained a value of Cs which is equal to 0.230 for the homogenous isotropic turbulences in inertial sub-ranges.

It has to be noticed that Cs isn't a "universal constant." The fact that CS has various values is a result of the average flow strain or shear which indicated the fact that the smaller eddies' behavior isn't of the same universality like it has been initially assumed. Another Cs value of about 0.10 was obtained for yielding quite good results for many different flow values and this value is utilized in the existing computing codes.

6. REMARKS ON THE LES

The large eddy simulation was introduced in 1960's; none-the-less, the computational power for the processing this model has not been provided available till lately for the problems of industrial relevance. The intrinsic LES's unsteady nature results in a considerably greater computation demand compared to the computation demand that are required by the conventional methods of RANS. LES is efficient in resolving specific time dependent turbulence characteristics without additional equations because it is intrinsic in its own formulation. LES provides more information about the average flow and their solved fluctuation statistics. Incorporating the LES codes in the software which is commercially available has only become lately accessible to engineering communities. The research and development pace which is based on this model is going to raise as with the increase in the power of the computational resources. Engineers will be more aware about the benefits of LES approach to the modelling of the turbulence, with the publishing of more meaningful data [7].

7. MEAN VELOCITY OF WIND

Wind velocity at great height over the ground has been constant and recognized as gradient wind velocity, close to ground surface, wind velocity has been impacted through frictional forces resulting from terrain, and therefore there has been boundary layer in which wind velocity vary from 0 to gradient wind velocity as can be seen in Figure 2. The depth that is related to boundary layer (gradient height) depend on ground roughness. For instance, value regarding has been 457m with regard to large cities, 366m with regard to suburbs, 274m with regard to open terrain as well as 213m with regard to open sea [16].

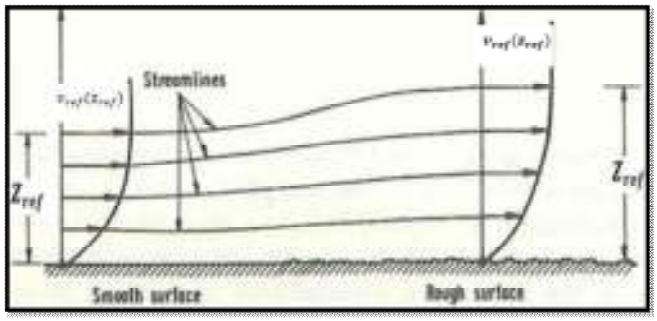

Figure 2: Change of Wind Velocity Distribution with Terrain Roughness. [14]

The wind's velocity averaged over single hour has been indicated as hourly mean wind speed $v(z)$. Power law can be seen in the Eq. (13) specified the mean wind velocity profile in atmospheric boundary layer as follows:

$$v(z) = v_{ref}\left(\frac{z}{z_{ref}}\right)^{\alpha} \quad (13)$$

In which $v(z)$ represent mean wind speed at height z above ground, z_{ref} Gradient height (boundary layer's thickness), typically taken to 10m, v_{ref} mean wind speed on the basis of building site, also α represent the power law exponent [14]. The logarithmic law has been indicated in Eq. (14) provides alternative description with regard to the mean wind velocity [14];

$$v(z) - \frac{1}{k}(v_*)\ln\left(\frac{z-d}{z_o}\right) \quad (14)$$

In which v_* represent friction velocity, *k* represents the von Karman's constant (equal to 0.4), z_o represents roughness length as well as d represent height of zero plane (in which velocity has been zero) above the ground. Typically, zero plane has been approximately 1 or 2 meters below average height regarding the buildings as well as the trees providing roughness. The typical values related to z_o, α and d have been provided in Table 1 [14].

Table 1: Typical Values of Terrain Parameters.

	Z_O(m)	α	d(m)
City Centers	0.7	0.23	15-25
Suburban Terrain	0.3	0.14	5-10
Open Terrain	0.03	0.11	0
Open Sea	0.003	0.09	0

The impact regarding ground roughness on mean wind profile can be seen in the Figure 3. Roughness will be

affecting power law exponent as well as boundary layer's thickness. As shown in the Figure 3, the thickness that is related to boundary layer as well as power law exponent will be increased with the surface's roughness. Therefore, velocity at all heights will be decreased with the increase in surface roughness. At the same time, with regard to all surfaces, gradient velocity is going to be he same. Therefore, in the case when wind's velocity regarding specific terrain has been identified, utilizing Eq. (13), Eq. (14), as well as Table 1 the velocity regarding certain terrain might be determined [14].

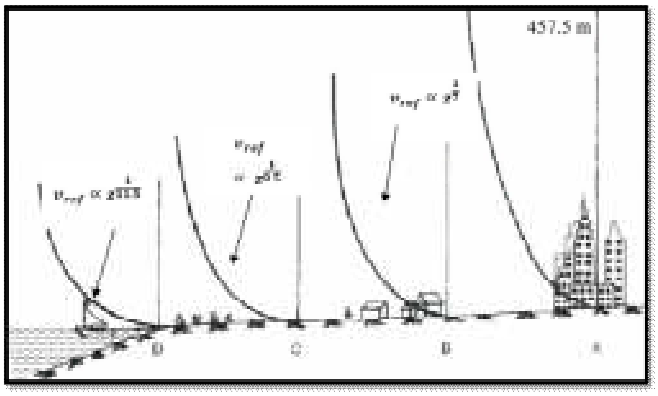

Figure 3: Variation of Wind Speed with Height. [16]

8. FORCES DUE TO UNIFORM FLOW

In the case when bluff body has been immersed in 2D flow as can be seen in the Figure 4, it has been subjected to net force in flow's direction (drag force) as well as force perpendicular to flow (lift force). Also, in the case when resultant force has been eccentric to elastic center, the body is going to be subjected to torsional moment. With regard to uniform flow, such forces as well as moment for each unit height regarding the object have been specified from [14].

$$F_D = \frac{1}{2}\,\rho\, C_D\, B\, [v(z)]^2 \qquad (15)$$

$$F_L = \frac{1}{2}\,\rho\, C_L\, B\, [v(z)]^2 \qquad (16)$$

$$F_T = \frac{1}{2}\,\rho\, C_T\, B\, [v(z)]^2 \qquad (17)$$

Where $v(z)$ represent the wind's mean velocity, ρ represent the air's density, C_D as well as C_L representing lift and drag coefficients, C_T represent the moment coefficient as well as B represent the object's characteristic length, like projected length normal to flow [14].

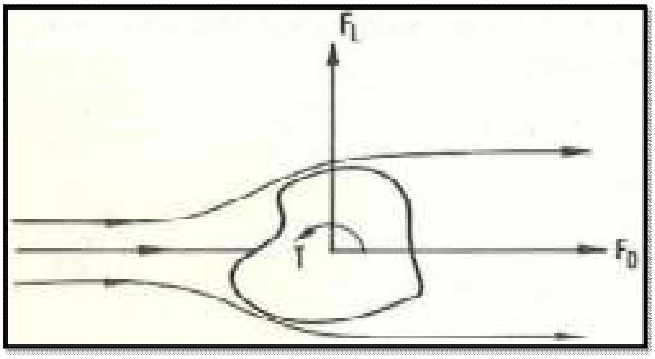

Figure 4: Drag, Lift Forces and Torsional Moment on an Arbitrary Bluff Body. [14]

9. CFD ANALYSIS OF THEORETICAL CASE STUDY HIGH-RISE BUILDING

The reason for choosing this model is the lack of sufficient information for the previously mentioned models in terms of structural design and specifications of materials used in construction and other things. The computational domain is defining regions in which flow field is numerically computed in assigned models. It must be sufficiently large for accommodating all related flow features which is going to have possible impact in changing the flow field's characteristics [22]. The building geometry with regard to the computational domain has been on the basis of the wind tunnel scaling regarding examining prototype structure. With regard to presented model, case study building has been square structure which has dimensions of 30 meters (B) by 30 meters (W) in plan form, also has the height of 200 meters (H) for the purpose of being one of the high-rise buildings. Such structure had ratio of height to base (6.67) which made it fall in slender structure's category. Generally, the slender structures have been massively impacted through lateral loading, also engineers in the case of designing these structures which are recognized for having high sensitivity to the lateral loading must be taking further diligence.

Wind tunnel scale has been selected as 1:400, since this is normal in industry practices to apply such factor between prototype as well as the model studies. With regard to the condition of selecting building, dimensions will be reduced to 0.075 × 0.075 × 0.5 meters. The constant 'B' in research has been determined to be 0.075 meters on the basis of scaling ratio. The already indicated constant has been applied as typical variable for describing all model's geometric properties.

10. COMPUTATIONAL DOMAIN AND MESH SCHEME

Computational domains, coordinate systems and boundary conditions used to analysis the flow around the building models are shown in the Figure 5. The dimensions of computational domain have been (29Bx17Wx4H m3) for the purpose of minimizing the blockage effect. The building is

putted in the computational domain in two ways depending on the distance between the building and the inlet of wind velocity as shown in the Figure 5. The unstructured tetrahedral mesh scheme is applied in this study as shown in the Figure 6. The number of elements for case study building case1 is about 720x103. In addition, the number of elements for case2 are 730x103.

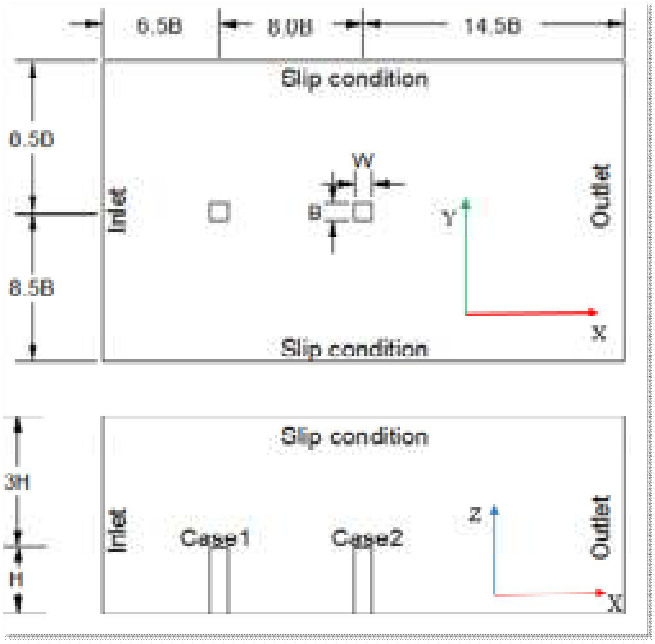

Figure 5: Computational Domains as well as Boundary Conditions.

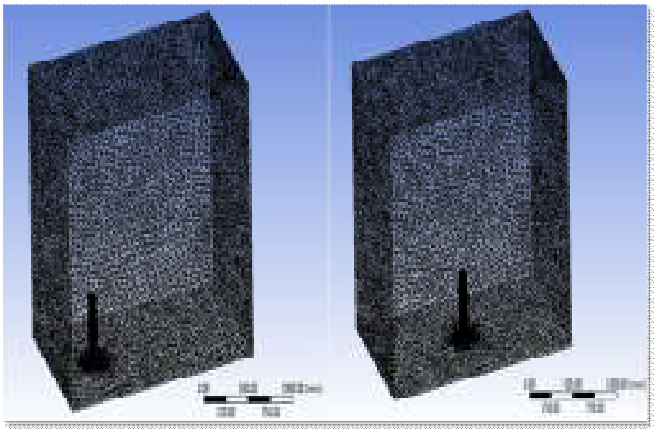

Figure 6: Mesh Generation.

11. TURBULENCE MODELS AND ANALYSIS METHODS

Most of buildings are in bluff body shape. Furthermore, it is extremely complex to determine precisely flow field because flows around buildings become of the extremely complex nature of separation, reattachment, wake, and unsteadiness [15]. In analysis of case study, the researcher uses the standard k-ε model for case1 as well as case2, also using LES for case1. LES can be considered as multi-scale computational method which provide comprehensive approach to capture unsteady flows. Using LES as one of the wind load evaluation tools was importantly enhanced recently with the use of numerical methods. LES are of high importance in the future related to computational wind engineering for which the turbulent flow vital. With regard to the presented work, Smagorinsky- Lilly subgrid-scale has been applied. Discretization that is related to convective terms central difference approach provides high precision in the case when put to comparison with upwind approaches. SIMPLE algorithm has been utilized for pressure-velocity coupling, also it is generally utilized in the standard k-ε as well as the LES simulations. The standard initialization was used for these analyses. All simulation have been carried out by utilizing two (DELL) laptop with Processors (CORE i5-2430M CPU @ 2.40 GHz) and (CORE i7-6500M CPU @ 2.50 GHz). The time step chosen for the LES was $1x10^{-3}$ seconds with 5 sub-iterations per time step and 5000 iteration for standard k-ε. Along with the already mentioned specifications, UDF according to computer C language has been written for simulating the required wind profile, which is based on the terms that have been already indicated. The code has been written for accommodating 3D model and it has been provided in the Appendix A. The power law was using in the inlet wind velocity as shown in the Figure 7.

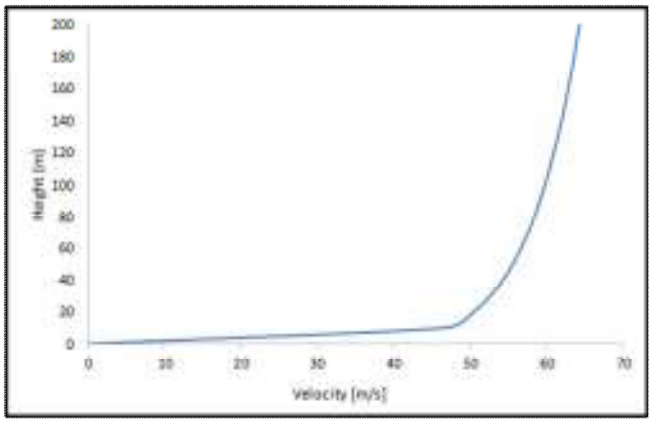

Figure 7: Velocity Inlet.

12. DYNAMICS ANALYSIS OF HIGH-RISE BUILDING CASE STUDY

The structure that has been specified in the presented work has been reinforced concrete that consist of fifty stories. Building's overall plan dimensions have been 30m by 30m consisting of six bays in horizontal direction x as well as five bays in y directions. The building has been two hundred meters over the ground level. The building floors consist of reinforced concrete beams with concrete slab. Column spacing has been five meters center-to-center in x direction as well as six meters center-to-center in y direction. Story height

has been four meters. Yet, Figure 8 show general framing plan regarding structure in distinctive views. Wind resistance structure contained shear walls from building's base to the full height of it. With regard to such systems, generally the shear wall will carry 85-95% of lateral load.

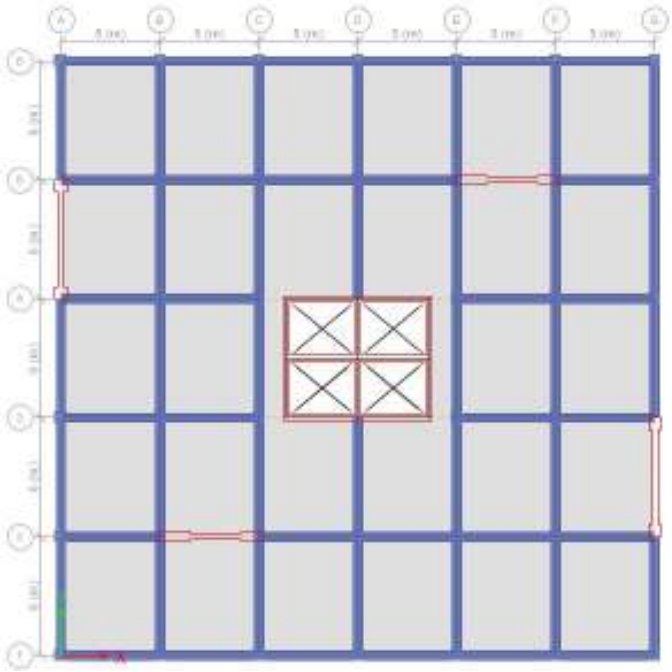

(a) Floor Plan Framing.

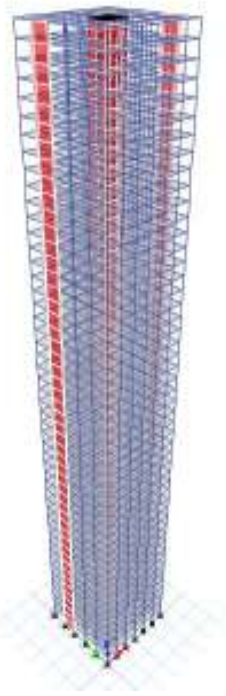

(b) Discretized FEM Model 50-Story.

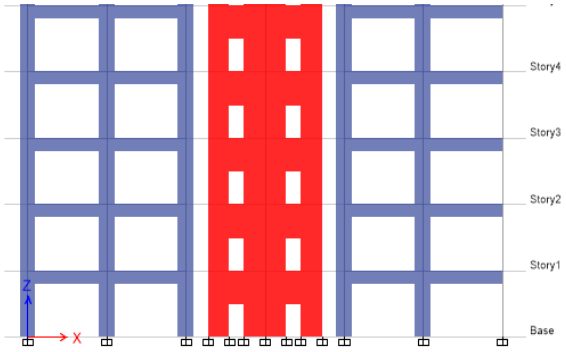

(c) North Elevation Framing.

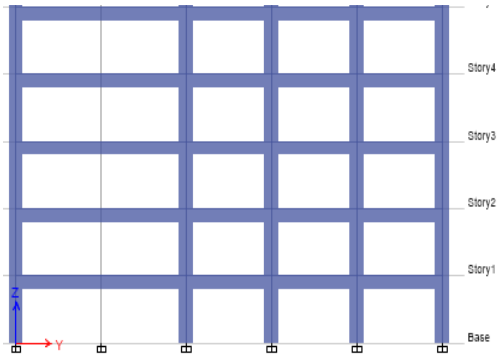

(d) East Elevation Framing.

Figure 8: Framing Model regarding 50-story Building Applied in This Work.

A frame has been developed as a moment resisting that contains vertical as well as horizontal components which have been connected in planar grid form. Such system majorly resists via member's flexural stiffness. Contra flexure's point will be typically found near midpoint regarding columns and beams. Typically, frame's deformation will be induced through shear-sway, also to some extent through column shortening. A few of the benefits to use such systems are its flexibility in the architectural planning. Furthermore, the size regarding members utilized in the moment resisting frame has been regularly maintained through the stiffness characteristics instead of strength. Element's stiffness majorly controlling suitable lateral drifts with regard to tall structures. The response of structures has been majorly considered as function of beam and column stiffness. Furthermore, with regard to the moment resisting frames, the column member's size will be reduced in size in the case when high levels have been achieved in building that is considered to be in proportion to lateral shear. The technological advances in computer field enabled more effective analysis regarding indeterminate moment frames. Certain method of optimization has been applied for determining the most effective distribution regarding the material of specific deformation limit analysis. The reinforced concrete frames were positive aspect where connections have been monolithically casted that have been

used for the moment resisting systems. Furthermore, improvements in testing caused conclusions in enhanced characteristics of concrete, more reinforcement requirements with regard to ductility's enhancements, as well as more effective frame forming approaches which will be applied in field.

13. ASSIGNED LOADING AND SECTION PROPERTIES TO HIGH-RISE BUILDING MEMBERS

The Assumed loads acting in structure are presented in Table 2 .Wind loading utilized on building's analysis has been from CFD wind analysis, where this wind load was exported from ANSYS to ETABS. The building was assumed to exist in Iraq, Baghdad in a flat open terrain region. Building's function has been suggested as office high-rise.

Table 2: Assumed Loads Acting on Structure.

Description	Type	Magnitude
Dead Load	D.L	(Member Size x Unit Weight) kN/m^2
Superimposed Dead	SDL	1 kN/m^2
Live Load	L.L	4.79 kN/m^2
Floor Cover	F.C	1 kN/m^2
Walls	D.L	[(Floor height - Beam depth) x wall thickness x Unit Weight] kN/m
Wind Loads	W.L	From ANSYS

On the basis of ASCE7/ACI318, there have been majorly 7 load combinations which might be utilized for strength design approach. Foundations, components, as well as structures have been needed to be developed so that their strength will be equal or more in comparison to the impacts regarding the factored load with regard to the presented combinations:

1) 1.4 D

2) 1.2 D + 1.6 L + 0.5 (Lr or S or R)

3) 1.2 D + 1.6 (Lr or S or R) + (L or 0.5W)

4) 1.2 D + 1.0 W + L + 0.5 (Lr or S or R)

5) 1.2 D + 1.0 E + L + 0.2 S

6) 0.9 D + 1.0 W

7) 0.9 D + 1.0 E

A lot of combinations have been created because studying the wind impact in multiple directions acting along buildings. This is going to provide analysis related to loads act overall structure. On the basis of such information, members could be developed to account for worst case bending, torsional, as well as shearing conditions regarding loading that is experienced through structure. Concrete building has been developed after taking into account recent standards. The building has been sub-divided in to 5 categories in which distinctive section properties to structure's members have been set. The initial category has been concentrated along building's base region in which the majority of bending as well as the shearing loading has been concentrated. Furthermore, the fifth category has been located on last 10 floors regarding structure in which members tending to have small dimensions.

Table 3: Properties and Cross-section of Members along Structure's Height

Cat.	Floor No.	Elevation (m)	Column Design		Shear Wall		Beam Design		Slab Design	
			B x W (mm)	f'c (MPa)	Thick (mm)	f'c (MPa)	B x H (mm)	f'c (MPa)	Thick (mm)	f'c (MPa)
1	1 10	4 40	1000x1000 1000x1000	50 50	300 300	50 50	600x800 600x800	30 30	300 300	30 30
2	11 20	44 80	900x900 900x900	50 50	300 300	50 50	600x800 600x800	30 30	300 300	30 30
3	21 30	84 120	800x800 800x800	50 50	300 300	50 50	500x700 500x700	30 30	250 250	30 30
4	31 40	124 160	700x700 700x700	50 50	300 300	50 50	500x700 500x700	30 30	250 250	30 30
5	41 50	164 200	600x600 600x600	50 50	300 300	50 50	450x650 450x650	30 30	200 200	30 30

Table 3 is showing the columns having maximum cross section along height which is found in the section referred to as Category 1. Final column design arrived with the use of iterative process as well as being verified against ACI318-08 code requirements with the use of ETABS as structural analysis software. Furthermore, columns were designed after utilizing concrete with fairly compressive strength (f'c has been 50 MPa). Column's cross section along Category 5 levels has been considerably decreased by about 40% in the case when compared to base floor levels. Exterior as well as interior have been suggested to have equivalent dimensions through all the category levels for simplifying the computational design time. The reinforcement which has been defined for such model has been ASTM A615 Grade 60

as well as Grade 75 steel. The Grade 60 steel has been applied in designing slabs as well as beams. Grade 75 steel has been applied for designing shear walls and columns.

The beam design along building's height has been indicated to be majorly uniform due to the fact that bays' span has not been equal in transverse and longitudinal directions. Slab design has been distinctive along all the levels regarding building and has been indicated for providing rigid diaphragm actions on the structure. Shear wall has been developed to be (300mm) thick in addition to having compressive strength (50Mpa) along structure's full height.

14. MASS MODELLING

With regard to ETABS, weight and mass are serving distinctive functions. Mass will be applied for inertia in dynamic analyses, also to calculate built-in acceleration loads. The weight has been a load which specified and assigned to at least one member, and might be utilized to at least one load case. ETABS provides 4 distinctive approaches, displayed in interactive box below, for generating mass matrix as exhibited in Figure 9.

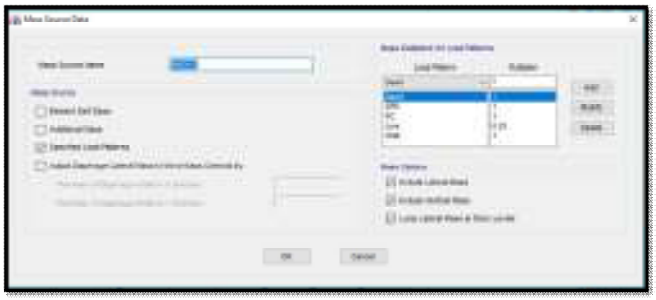

Figure 9: Panel of Define of Mass Source.

With Element Self Mass and Additional Mass source, the program applies these mass specifications:

1. Mass density indicated for the materials.

2. More line mass allocated to the frame or cable objects.

3. More area mass allocated to the area objects.

4. Mass indicated for the link properties.

5. Mass directly allocated to joints.

With the specified Load patterns source, the mass might be estimated from scaled combination regarding the load patterns. At the same time, absolute value related to net load act in the global Z direction has been divided through acceleration because of gravity, in current units, is applied for mass in 3 translational directions.

In this work, the applied load that consists of dead and live loads were utilized via specified Load patterns source.

15. TIME HISTORY FUNCTION

In this part of the program, the wind function is defined for dynamic analysis, where time function has been utilized for defining temporal variation in the wind pressure as shown in the Figure 10. In this study, the sine function is used by ETABS program.

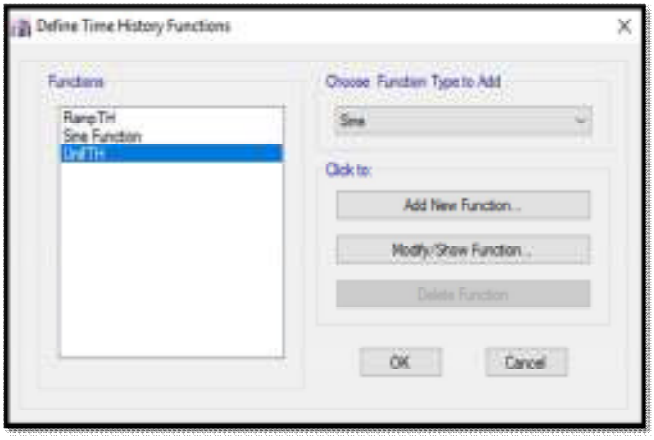

Figure 10: Panel of Time History Function.

16. LOAD CASE DEFINITION

Lastly, spatial and temporal time variations have been merged together via load case definition as shown in the Figure 11. After that analysis, the case study building and then the result can be seen after analysis complete. This analysis has been carried out by utilizing (DELL) laptop with Processor (CORE i5-2430M CPU @ 2.40 GHz).

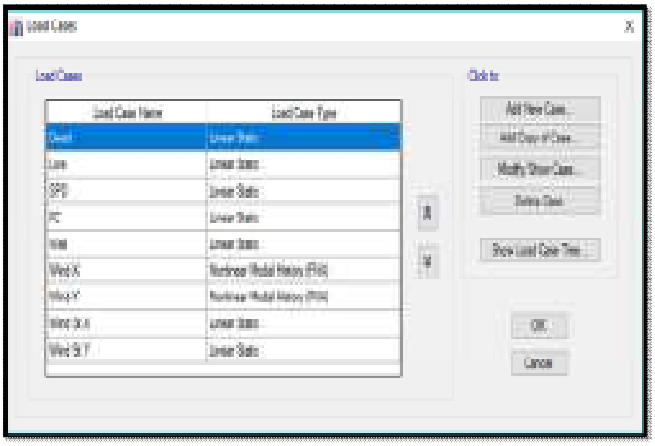

Figure 11: Panel of Load Case.

17. THE VALIDATION OF MODEL

The validation regarding the model that is examined through the user of CFD has been extremely essential to conduct. Validation has been considered as an approach to determine the degree to which a model has been precise representation regarding physical world from perspective related to prepared model usages. The major approach for achieving comfort with model of CFD is making direct comparisons to experimental or published data. With regard to this work, a lot of physical researches were conducted in fluid flow around the square geometries.

Any one of the objects in which the fluid has been moving around it is going to experience drag that could be specified as net force in direction regarding flow because of pressure as well as the shear force act on surface related to obstacle. Generally, object with certain shape could be specified through its drag coefficient, C_D.

Furthermore, the drag coefficient can be considered as function regarding dimensional parameters like relative roughness, Mach number, Reynolds number, as well as Froude number. Square cylinder was indicated to be C_D value regarding the approximately 2.10 which has been derived from the experimental study as indicated in the Table (4).

Table 4: The Experimental Data as well as Derived Quantities with regard to different Cross Sections. [1]

Source	Re	C_D
Store belt bridge	2000000	0.60
Store belt bridge	50000	0.68
Circular cylinder	4500	0.70
Tacoma bridge	600000	1.25
Square cylinder	176000	2.04
Square cylinder	100000	2.05
Square cylinder	13000	0.216
Inclined square cylinder	600000	2.4

Model's validations have been conducted with fluid behave in turbulent way due to the fact that its Reynolds number has been in order of 2 x 10^5. The details that are related to model set up could be indicated in the Appendix B since in consists of all approaches and means as input parameters with regard to model in the ANSYS Fluent. Figure 12 will show time-dependent plot that is related to drag's coefficient which square structure has. The comparison that is related to coefficient of the drag with computed through numerical CFD model has been in accordance to the experimental data as well as [2].

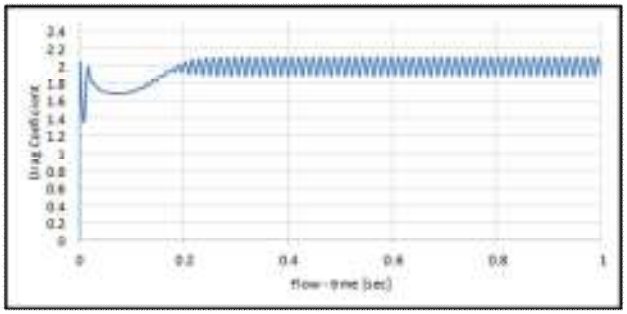

Figure 12: Drag Coefficient Curve for SST k-ω Transient Model.

Furthermore, CFD model has been programmed for measuring lifts coefficient, that act in perpendicular direction to drag forces as can be seen in Figure 13.

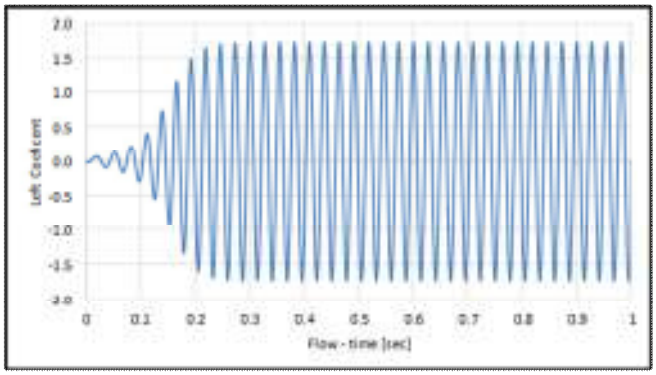

Figure 13: Lift Coefficient Curve for SST k-ω Transient Model.

18. THE DESIGN PRESSURE, FLOOR-BY-FLOOR LATERAL LOAD, STORY SHEAR AND OVERTURNING MOMENT RESULTS OF HIGH-RISE BUILDING CASE STUDY

18.1 Velocity Inlet

User defined function (UDF) which is on the basis of computer C language has been written through the researcher for the purpose of simulating the required wind profile. The profile has been in agreement with the suggestion previously indicated. The code has been written for accommodating 3D model, also it is provided in Appendix A.

The Figure 14 can be considered as computer output that is related to velocity profile as written through the code which is written through the researcher. It has been on the basis of power law, also it carried exponent regarding 1/9.5 as per case study model conditions as well as the ASCE 7-10 recommendations.

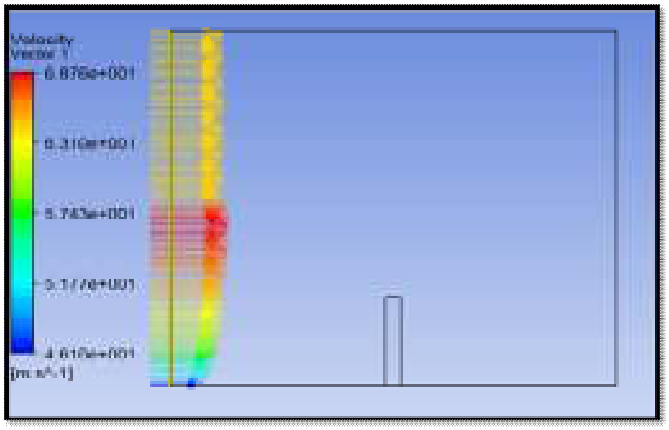

Figure 14: Wind Profile Generated in Computer Domain.

18.2 LES Result for Case2 Analysis

The objective of this analysis is to investigate applicability of loads computed by CFD to design building structures. Thus, the results of the CFD simulations for high-rise building model mentioned previously are presented in Figure 15 to Figure 18 comparisons with those obtained by the international building design codes.

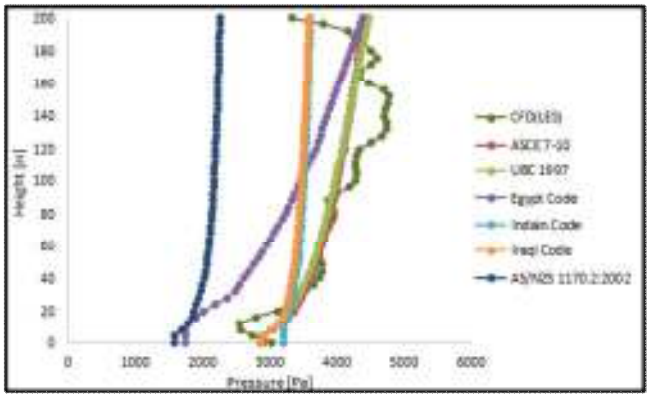

Figure 15: Design Pressure Comparison between CFD and Building Codes.

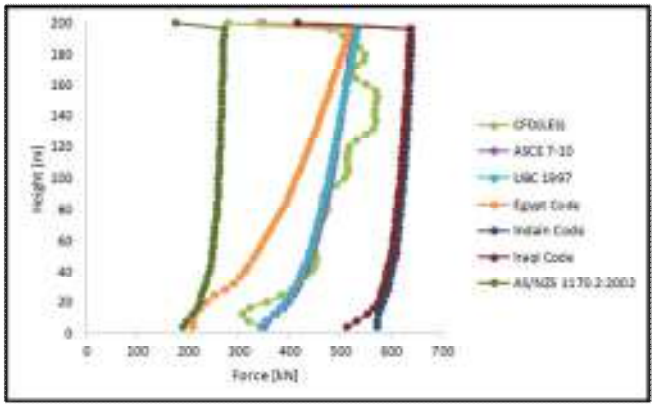

Figure 16: Floor-by-Floor Lateral Load Comparison between CFD and Building Codes.

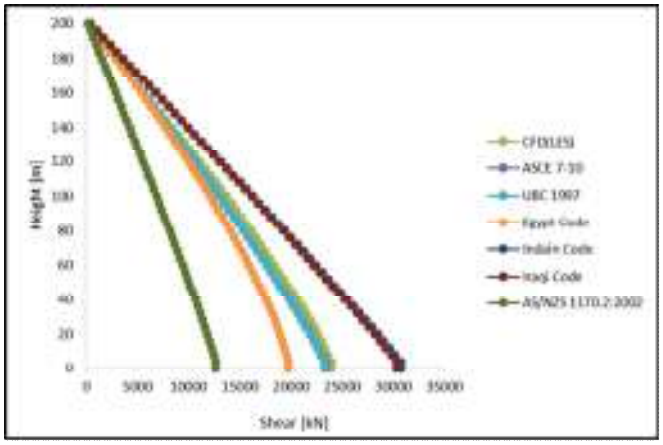

Figure 17: Story Shear Comparison between CFD and Building Codes.

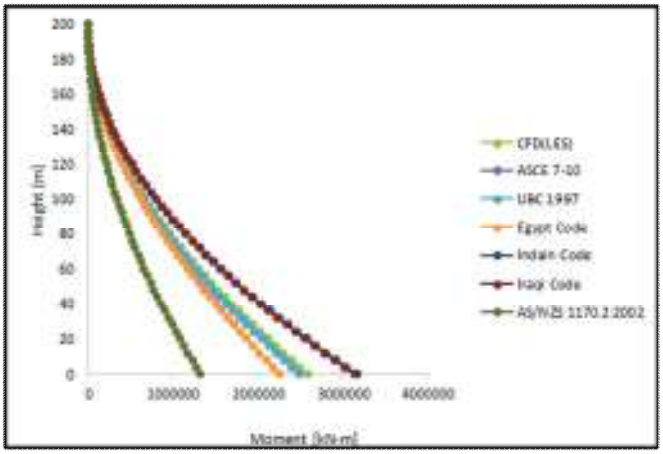

Figure 18: Overturning Moment Comparison between CFD and Building Codes.

The design pressure, floor-by-floor lateral load, along-wind shear forces and overturning moments obtained by CFD simulations for the high-rise building model compared with those of ASCE 7-10, Indian code, Iraqi code, Egypt code, UBC 1997 and AZ/NZS 1170.2:2002, as shown in Figure 15 to Figure 18. The story shear forces and overturning moments calculated from CFD simulations are in the qualitative agreement with building code. The result of CFD simulation are in between the building codes. It is shown that the Indian code has the most conservative values while values of UBC and ASCE have similar distributions in story shear forces and story overturning moments.

18.3 The Standard (k-ε) Result for Case1 and Case2 Analysis

The objective of this analysis is to investigate applicability of loads computed by CFD to design building structures. Thus, the results of the CFD simulations for high-rise building model mentioned previously are presented in Figure 19 to Figure 22 shown comparisons with those obtained by the international building design codes.

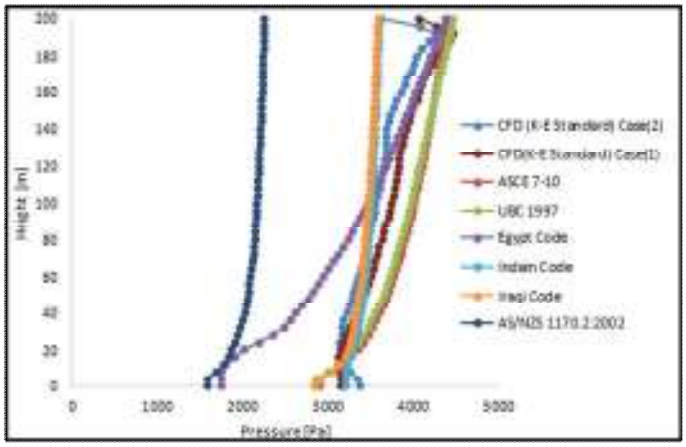

Figure 19: Design Pressure Comparison between CFD and Building Codes.

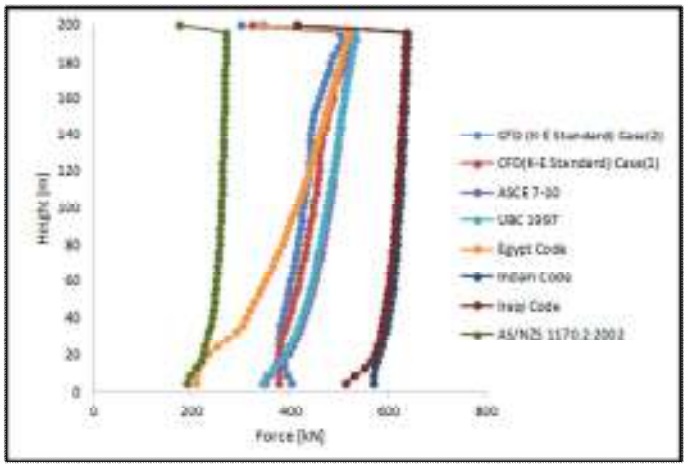

Figure 20: Floor-by-Floor Lateral Load Comparison between CFD and Building Codes.

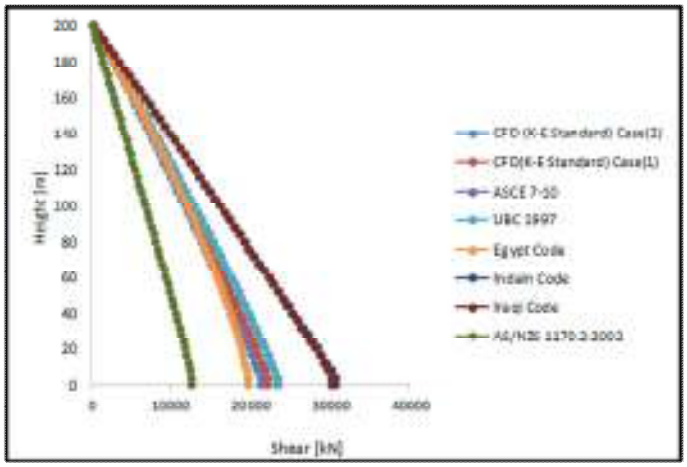

Figure 21: Story Shear Comparison between CFD and Building Codes.

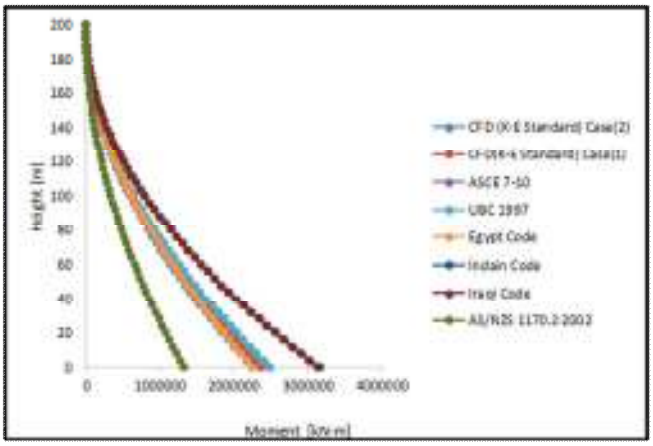

Figure 22: Overturning Moment Comparison between CFD and Building Codes.

The design pressure, floor-by-floor lateral load, along-wind shear forces and overturning moments obtained by CFD simulations for the high-rise building model compared with those of ASCE 7-10, Indian code, Iraqi code, Egypt code, UBC 1997 and AZ/NZS 1170.2:2002, as shown in Figure 19 to Figure 22 above. The story shear forces and overturning moments calculated from CFD simulations with case1 and case2 are in the qualitative agreement with building code and the results of this method are batter from LES method. The result of CFD simulation are in between the building codes. It is shown that the Indian code has the most conservative values while values of UBC and ASCE have similar distributions in story shear forces and story overturning moments. The pressure contour for Case1 and Case2 analysis are presented in Figure 23.

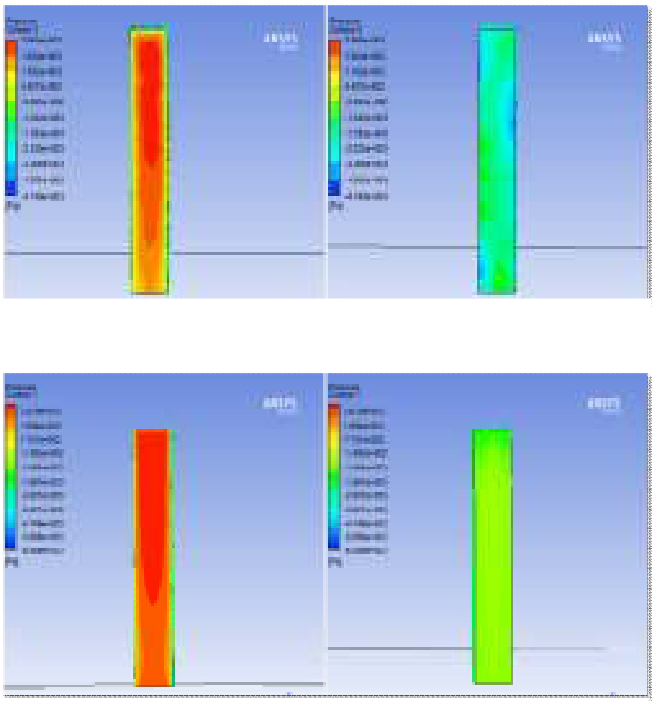

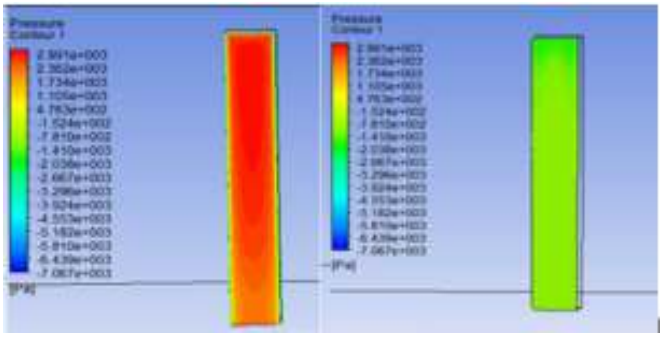

(a), (b) LES Case2, (c), (d) Standard (k-ε) Case1 and (e), (f) Standard (k-ε) Case2

Figure 23: Pressure Contour for Windward and Leeward Faces.

19. DYNAMIC ANALYSIS OF HIGH-RISE BUILDING OF THEORETICAL CASE STUDY

19.1 Vibration Modes of Modeled building

A building has set of the modes shape which is majorly on the basis of the boundary conditions, mass of materials, as well as the structure stiffness. Each one of the buildings has some modes or ways, where it might be naturally vibrating or through dynamic forces such as earthquake load or wind load. With regard to each one of the modes, the structure might be naturally oscillating back and forth with specific distorted shape which is recognized as the mode shape. A building could be created for swaying at other frequencies related to vibration with distinctive mode shapes in comparison to its fundamental (lowest) frequency in the case when loading happens at distinctive levels. A major function which impact building's stiffness is its height. Thus, tall buildings have tendency toward having high flexibility as well as high susceptibility to low frequencies. The results that are provided in Figure 24, Figure 25 and Figure 26 have been arrived with the use of eigenvector modal analysis code that is imbedded in ETABS program that follow a theory provided in Chapter 2. Eigenvector analysis will be determining undamped free-vibration mode frequencies and shapes of system. Analysis has been limited through a user to 6 vibration modes, which could be recognized in these simplified terms. The initial mode has been translational in direction. The second mode has also been translational. The third mode has been torsional mode. The rest of high modes have been generally combination regarding the first 3. With regard to the study of fifty mode shape with regard to building, may be the first 5 to 6 or more modes provide some information related to structural engineer with regard to design criteria.

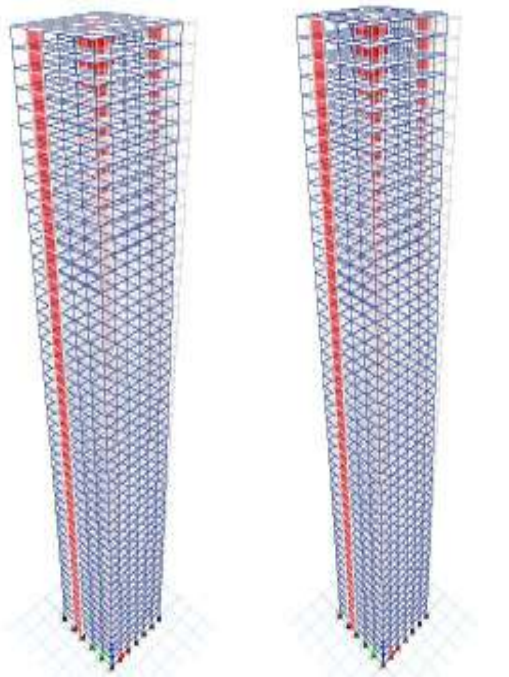

(a) Mode 1 – f = 0.118 Hz (b) Mode 2 – f = 0.127 Hz

Figure 24: First and Second Modes of Vibration of Tall Structure.

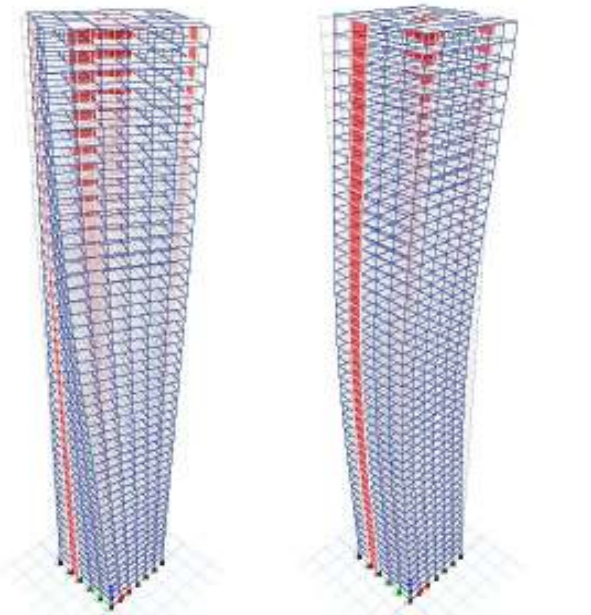

(a) Mode 3 – f = 0.206 Hz (b) Mode 4 – f = 0.391 Hz

Figure 25: Third and Fourth Modes of Vibration of Tall Structure.

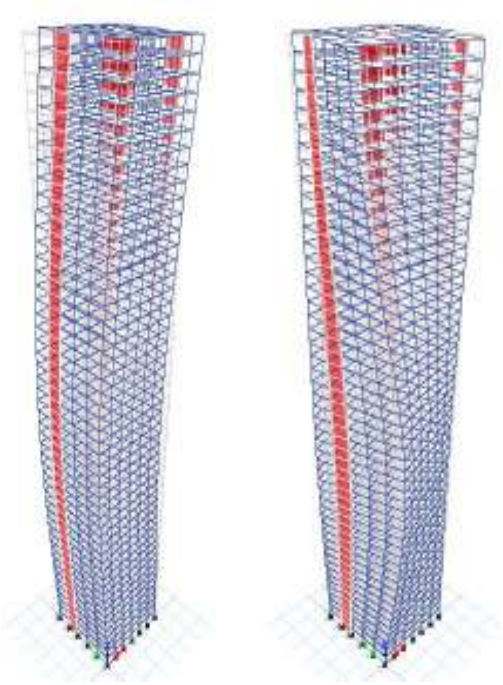

(a) Mode 5 – f = 0.438 Hz (b) Mode 6 – f = 0.564 Hz

Figure 26: Fifth and Sixth Modes of Vibration of Tall Structure.

With the aim that is related to the mitigate vibrations, an engineer has the ability of making a lot of changes in building design for avoiding likely resonance between lateral loading and structure. In the case when structure vibrate at frequency that provide sensitivity to humans, the engineer will have the ability of altering structures period regarding vibration through changing its stiffness of mass. This could be conducted via: 1) stiffening structural members, 2) increase the number of columns, as well as 3) reducing decking material to lightweight component. Furthermore, all the structures have certain inherent damping. More approaches could be applied where damping could be elevated and therefore dissipating energy in the case when a structure move. Yet, using mechanical damping devices is of high financial costs.

20. CONCLUSION

We can summarize what we have reached in this paper to some very important conclusions in civil engineering. The theory of computational fluid dynamics can be used in the analysis of high-rise building for wind load, where the results extracted through the CFD proved that there is a very large agreement between them and the results extracted from the building codes. The results show that the computational fluid dynamics can be used instead of costly wind tunnel test as well as instead of on-site calculations or building codes. Where it is possible through CFD to make a full report on the results obtained easily. Through the computational fluids dynamics, it is possible to know the distribution of pressure and the distribution of wind on a high building and to know the critical points that are useful in designing tall buildings in the future. The analysis of this building dynamically explains how the wind affects the high building and knowing the frequency of the building as it is a very important point in the design process. The structural designer must do all the necessary procedures to make the building safe for housing and not failable as possible in the future. It should be noted that this type of study needs to be further developed, i.e. by other indication it needs more research in this aspect in the future.

REFERENCES

[1] Ahlborn, B., Seto, M. L., Noack, B. R. (2002). “On drag, Strouhal number and vortex-street structure,” Japan Society of Fluid Mech., Vol. 30, 379-399. https://doi.org/10.1016/S0169-5983(02)00062-X

[2] Assaad B. “Wind Effect on Super-Tall Buildings Using Computational Fluid Dynamics and Strctural Dynamics,” 13 Ekp 1576–1580 (2015).

[3] Dagnew, A. (2012). Computational Evaluation of Wind Loads on Low- and High- Rise Buildings".

[4] Dagnew, A. K., Bitsuamalk, G. T., & Merrick, R. (2009). Computational evaluation of wind pressures on tall buildings. Americas Conference on Wind Engineering.

[5] Davidson, L. (2019). Fluid mechanics, turbulent flow and turbulence modeling. Chalmers University of Technology, Goteborg, Sweden, 1–270.

[7] Versteeg and Malalasekera. (2007). Introduction to Computational Fluid Dynamics. In Introductory Fluid Mechanics.

[8] Hinze, J. O. (1975). Turbulence. McGraw-Hill Publishing. New York, N.Y.

[9] Inc. ANSYS. (2014). Fluent – Theory Guide. Canonsburg, PA.

[10] Jeong, J., & Choi, C.-K. (2008). Comparison of Wind Loads on Buildings using Computational Fluid Dynamics, Design Codes,\rand Wind Tunnel Tests. The 4th International Conference on Advances in Wind and Structures (AWAS’08), (May 2008).

[11] Menter, F. (1994). Two-equation Eddy-Viscosity Turbulence Model for Engineering Applications, AIAA J., Vol. 32(8), 1598-1605.

[12] Shireen T. Saadullah and James H. Haido. (2017). Wind Analysis of Tall Building in Duhok City Using Computational Fluid Dynamic (Cfd). The Journal of The University of Duhok, 20(1), 520–536. https://doi.org/10.26682/sjuod.2017.20.1.46

[13] Smagorinsky, J. (1963). "General Circulation Experiments with the Primitive Equations. I. The Basic Experiment," Month. Wea. Rev. 91. 99–164.

[14] T. Balendra. (1993). "Vibration of Buildings to Wind and Earthquake Loads," Springer. https://doi.org/10.1007/978-1-4471-2055-1

[15] Tamura, T., Kawai, H., Kawamoto, S., Nozawa, K., Sakamoto, S., and Ohkuma, T. (1997). "Numerical prediction of wind loading on buildings and structures – Activities of AIJ cooperative project on CFD",. Journal of Wind Engineering and Industrial Aerodynamics, 67–78, 671-685.

[16] Taranath, B. S. (2005). Wind and Earthquake Resistant Buildings – Structural Analysis and Design. CRC Press, Taylor & Francis Group, Boca Raton, FL. https://doi.org/10.1201/9780849338090

[17] W. S. Karrar et al. Comparing of Wind Pressure of a High-Rise Building in Baghdad City between Wind Tunnel and CFD Results. International Journal of Latest Engineering Research and Applications (IJLERA) . Vol. 05, Issue 01, January 2020.

[18] W. S. Karrar et al. "Comparison of Pressure Results between Wind Tunnel and CFD Simulation for University Baghdad Tower Building," International Journal of Modern Research in Engineering and Technology (IJMRET). Vol. 05, Issue 03, March 2020.

[19] W. S. Karrar et al. "Wind Pressures Comparison between Wind tunnel and CFD on Square and Triangle Shapes Tall Buildings," International Journal of Innovations in Engineering Research and Technology [IJIERT]. Special Issue-2020 15th June.

[20] W. S. Karrar et al. "A Pressure Comparison of Tall Building of Baghdad University Tower and Baghdad Tower between Wind tunnel and CFD," International Journal of Creative Research Thoughts. Issue 7 , Volume 8. July.

[21] Aaron Don M. Africa, Lourdes Racielle Bulda, Emmanuel Del Rosario, Matthew Zandrick Marasigan, Isabel Navarro Calculating Characteristic Impedance Without Using Symmetricity of Rectangular Coaxial Line. International Journal of Emerging Trends in Engineering Research (IJETER) Volume 7, No. 8 August 2019. https://doi.org/10.30534/ijeter/2019/06782019

[22] Mohd Fakri Muda , Saffuan Wan Ahmad , Fadhluhartini Muftah , Mohd Syahrul Hisyam Mohd Sani. Mechanical Behaviour of Mortar Made with Washed Bottom Ash as Sand Replacement //International Journal of Emerging Trends in Engineering Research Volume 7, No. 9 September 2019.

[22] Franke, J., Hellsten, A., Schlunzen, H., Carissimo, B., (2007). Best Practice Guideline for the CFD Simulation of Flows in the Urban Environment, COST Action 732.

Appendix A

User Defined Function for 3D Wind Profile in C-language

```
#include "udf.h"
DEFINE_PROFILE(x_velocity,thread,index)
{
real x[ND_ND];
real z;
face_t f;
real H;
real del;
real zref;
real vref;
H=0.5;
del=2*H;
zref=0.025;
vref=47;
begin_f_loop(f,thread)
{
F_CENTROID(x,f,thread);
z=x[2];
if (z<=del)
F_PROFILE(f,thread,index)=vref*pow((z/zref),(1.0/9.5));
else if (z>del)
F_PROFILE(f,thread,index)=64.425;
}
end_f_loop(f,thread)
}
```

Appendix B

The Properties of the $K - \omega$ SST Analysis Model

The plan form of the geometric properties can be seen in (Figure B-1). The overall computational domain was 2.1 × 4.7 where the structure was centered at 1.05 from the inlet and 1.05 from the south wall condition. A distance of 3.6 in the downstream direction was chosen to allow for the reduction of the disturbances experienced by the flow.

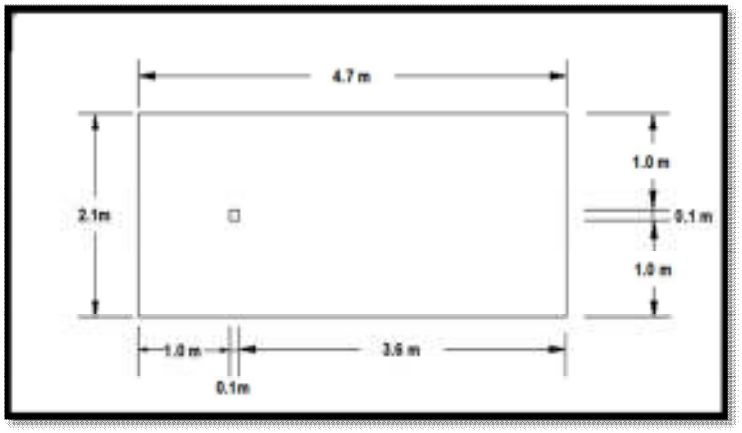

Figure (B-1): 2D Plan Dimensions.

The mesh properties can be shown in the (Figure B-2).

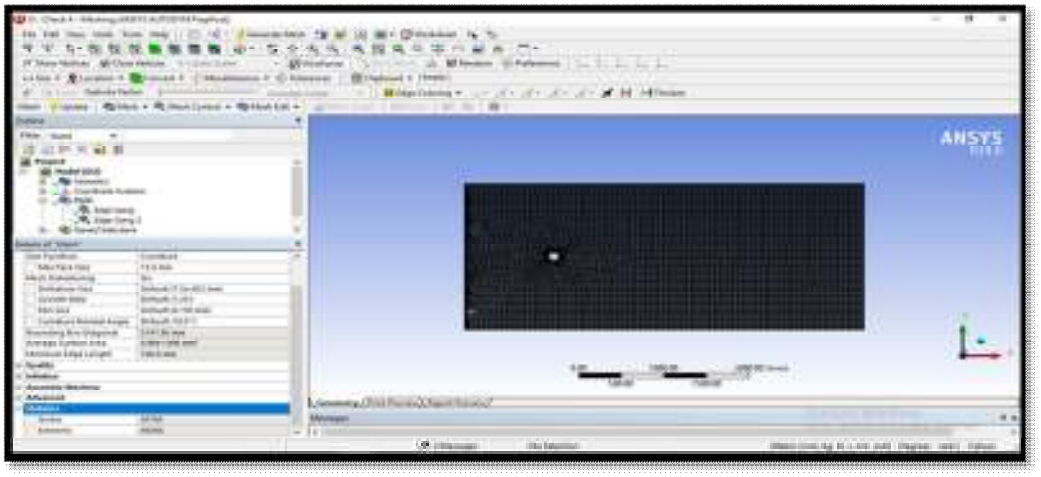

Figure (B-2): The Mesh Generation

The boundary condition can be seen in the (Figure B-3). The inlet velocity was 29.6 m/s and the outlet pressure was zero pressure. Wall was symmetry. The Turbulent intensity was 14.1% and the turbulent length scale was 0.613m for this status. The area and the length in the reference value were 0.1.

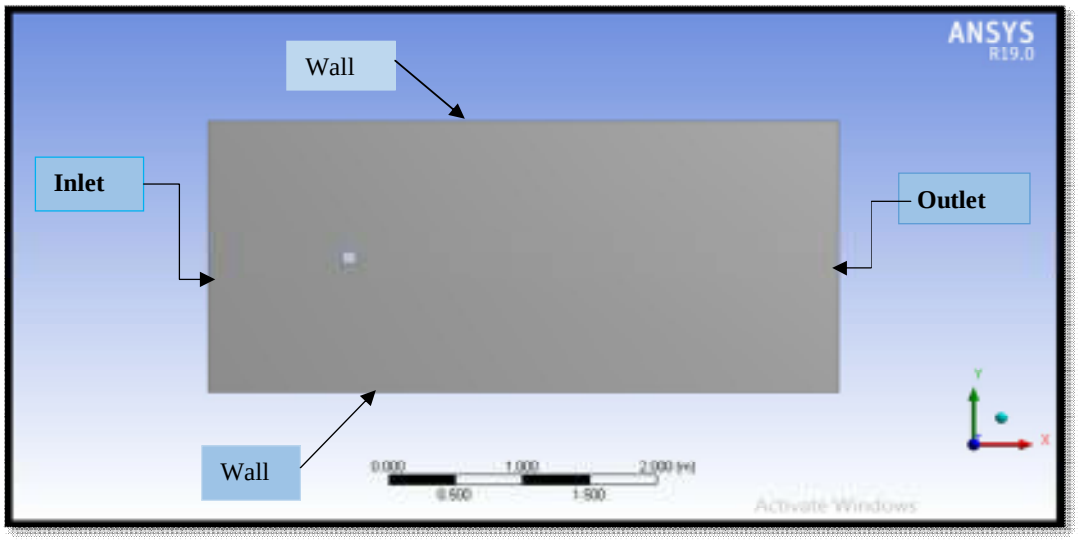

Figure (B-3) :2D Plane Boundary Conditions

The time in this case is transient, in the other hand the iteration can be shown in the (Figure B-4). The initialization is hybrid.

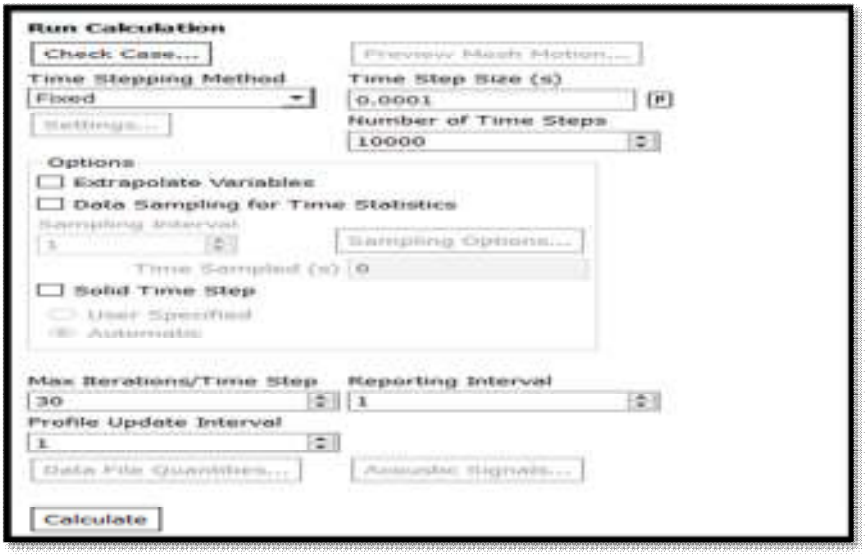

Figure (B-4) : Panel of the Iteration